

## Non-LTE Ionization and Energy Balance in High-Z Laser Plasmas Including Two-Electron Transitions

J. R. Albritton and B. G. Wilson

*Lawrence Livermore National Laboratory, L-41, P.O. Box 808, Livermore, California 94550*

(Received 26 January 1999)

We describe a new non-LTE average-atom-kinetics model of plasmas in which the two-electron transitions of autoionization and its inverse, resonant capture, play a dominant role in establishing ionization and energy balance. We show that, compared with a familiar collisional-radiative-equilibrium model for laser-produced gold plasmas: (1) the two-electron transitions force recombination of the plasma with decreasing density, and (2) the two-electron transitions nevertheless further act to greatly increase the radiative emissivity of the plasma.

PACS numbers: 52.25.Jm, 32.30.Rj, 52.55.Dy

The ionization state of laser-produced high-Z plasmas must often be modeled by a nonlocal thermodynamic equilibrium (NLTE) atomic kinetics scheme [1]. Typically this results from a weak and NLTE ambient radiation field, far from the free electron temperature. Furthermore, the collisions of the free electrons may not be strong enough to establish detailed balance of the bound-bound and bound-free electron transitions of the ions. The NLTE ionization state is then determined by the balancing of the strongest electron transition processes.

A familiar physical model is that of the collisional-radiative equilibrium (CRE) and its one-electron (1e) collisional and radiative bound-bound and bound-free transitions [2]. In a CRE model, and in a negligible radiation field, the plasma ionization state becomes independent of density with decreasing density as the balancing source and sink, radiative recombination and collisional ionization, respectively, both become proportional to the free-electron density. This is the well-known coronal limit.

Thompson scattering of probe pulses in recent laser-produced-plasma experiments [3] provide data which suggest that the CRE model requires improvement. Decreasing ionization was observed with decreasing density. Indeed, default radiation-hydrodynamics NLTE modeling, LASNEX/XSN [4,5], failed to satisfactorily simulate the observed plasma state, especially the behavior with electron density. On the other hand, practically prohibitive detailed-configuration-accounting NLTE modeling, LASNEX/DCA [6], gave quantitative improvement and qualitative agreement. The present report concerns a key feature implemented in LASNEX/DCA, and describes the first analytical and numerical results of its practically efficient formulation for implementation in models such as LASNEX/XSN.

We describe the NLTE modeling of plasmas in which the two-electron (2e) transitions of autoionization and its inverse, resonant capture, play an important role in establishing ionization and energy balance. We develop a new model suitable for application in situations where

detailed models are too complex or costly. We show that 2e transitions can dominate the ionization balance and force recombination of the plasma with decreasing density; we derive a new density scaling law which stands in contrast to the coronal limit and in concert with the recent experimental results. We also show that 2e transitions act to greatly increase the radiative emissivity and thereby increase the thermal cooling rate of the plasma; this has significant consequences for modeling the dynamics of laser plasmas.

For the purpose of instruction it is sufficient to consider a model system of ions possessing only two bound levels, an effective ground/inner level and an excited/outer level, denoted 1 and 2, respectively. An ionic configuration of integer level occupations is  $\vec{N} = (N_1, N_2)$ , and  $\vec{D} = (D_1, D_2)$  are the level degeneracies or maximum occupations. Heuristically, the plasma ionization state is determined by the large number of ions with at least partially filled inner levels, while the radiative emissivity is determined by the relatively small number of ions with electrons also in outer levels. That is, it is useful to consider configurations such that  $N_1 > N_2$ , so the ionization state  $Z^* = Z - (N_1 + N_2) \approx Z - N_1$ , depends dominantly on  $N_1$ . Similarly,  $D_1 > N_1$ , so the power emitted in spectral lines from spontaneous radiative decay transitions from level 2 to level 1,  $X_{21} \sim N_2(D_1 - N_1) \sim N_2 D_1 \sim N_2$ , depends dominantly on  $N_2$ . The occupations of the two levels act separately to control the plasma ionization and energy balance.

Figure 1 is a schematic illustration of a 2e autoionization transition, an event in which one electron falls down from level 2 to level 1, while another electron in level 2 receives the transition energy of the falling electron and jumps up into the continuum, that is, is ionized. If the initial configuration is  $(N_1, N_2)$ , then the final configuration is  $(N_1 + 1, N_2 - 2)$ . Note that a multiply excited ion is required,  $N_2 - 2$  non-negative, and that an inner vacancy must exist,  $(D_1 - N_1)$  positive.

Energy conservation in the 2e transition requires that the kinetic energy of the ionized electron is

$$\begin{aligned} \varepsilon_{\text{kin}} &= E_{\text{ion}}(N_1, N_2) - E_{\text{ion}}(N_1 + 1, N_2 - 2) \\ &\approx (\varepsilon_1 - \varepsilon_2) - \varepsilon_2 = \varepsilon_1 - 2\varepsilon_2. \end{aligned}$$

Here  $E_{\text{ion}}$  is the total energy of the bound electron configuration, and  $-\varepsilon_i$  are the energies (negative definite eigenvalues) of the bound levels;  $\varepsilon_1 - \varepsilon_2$  is the energy made available to the jumping electron, and  $\varepsilon_2$  is the minimum amount it must jump to reach the continuum.

$$\begin{aligned} \dot{F}(N_1, N_2) &= -F(N_1, N_2)A_{122}(N_1, N_2)(D_1 - N_1)N_2(N_2 - 1) \\ &+ F(N_1 - 1, N_2 + 2)A_{122}(N_1 - 1, N_2 + 2)[D_1 - (N_1 - 1)](N_2 + 2)(N_2 + 1). \end{aligned} \quad (1)$$

Here “dot” denotes the time derivative, and  $A_{122}$  is the  $2e$  transition rate for autoionization, reckoned according to the number of electrons and holes available to participate in a transition; these are the final factors in the transition terms above. The subscripting denotes the three levels involved in the  $2e$  transition, inner/outer/outer. Note that from  $A$  there is both a gain and a loss term to the configuration of interest, and that the sum over all occupations of the two terms vanishes, so that the total probability is conserved. Gains to a certain configuration are exactly losses from another, “adjacent,” configuration. Later in our development we include the inverse process of resonant capture, and then also the usual  $1e$  transitions. Finally, we show results from a complete multilevel model.

For our purposes LASNEX/DCA may be viewed as the direct treatment of Eq. (1) by including many configurations; construction of such a plasma ensemble can be a costly exercise. Here we describe the statistical treatment of Eq. (1); we formulate equations for the evolution of the average populations of the levels,  $P_1 = \langle N_1 \rangle = \sum_{\vec{N}} N_1 F(\vec{N})$  and  $P_2 = \langle N_2 \rangle = \sum_{\vec{N}} N_2 F(\vec{N})$ . This great

The  $2e$  transition is energetically allowed, or above threshold, when  $\varepsilon_{\text{kin}}$  is non-negative. Note that the inverse transition of free electron capture is a resonant process, involving a free electron of kinetic energy equal to the difference between the two ion configuration energies.

The kinetic equation governing the time evolution of the probability distribution of configurations of ions under  $2e$  autoionization transitions may be written as

reduction in the detail of the treatment yields a corresponding reduction in the effort required for its application; it further yields useful physical insight through the scaling laws able to be deduced.

We begin by multiplying Eq. (1) by  $N_2$  and summing over all  $\vec{N}$  to obtain the equation governing  $P_2$ . As is useful in demonstrating conservation of total probability, introduce the dummy indices  $N'_1 = N_1 - 1$  and  $N'_2 = N_2 + 2$  in the sum from the second term on the right-hand side (rhs) of Eq. (1) to obtain a partial term-wise cancellation with the first:

$$\dot{P}_2 = -2 \sum_{\vec{N}} F(\vec{N})A_{122}(\vec{N})(D_1 - N_1)N_2(N_2 - 1).$$

The terms proportional to the leading factor of  $N_2$  cancel; the surviving number minus two is the change in the upper level occupation upon an autoionization event.

Now suppose that  $A$  is slowly varying about its value at the mean occupations,  $A(\vec{N}) \sim A(\vec{P})$ , and remove that from the summand. Also write  $\vec{N} = \vec{P} + (\vec{N} - \vec{P}) = \vec{P} + \Delta\vec{N}$  to perform the remaining sums “exactly.”

$$\dot{P}_2 = -2A_{122}(D_1 - P_1)[P_2(P_2 - 1) + \langle \Delta N_2^2 \rangle].$$

It turns out that if  $A$  is effectively independent of occupation, then  $F$  is a separable function of  $N_1$  and  $N_2$ ,  $F(N_1, N_2) \sim F_1(N_1)F_2(N_2)$ , so that the “cross”-correlations vanish,  $\langle \Delta N_1 \Delta N_2 \rangle \sim 0$ , and only the “self”-correlations,  $\langle \Delta N_2^2 \rangle$ , survive. This is the familiar physics of the noninteracting Fermion model of systems of bound electrons. The self-correlations are well known

$$\langle \Delta N_2^2 \rangle = P_2(D_2 - P_2)/D_2$$

and combine conveniently with the first term in the square brackets.

$$\dot{P}_2 = -2A_{122}(D_1 - P_1)P_2^2(1 - 1/D_2).$$

The retention of the self-correlation term is essential in obtaining a model which obeys the LTE limit. In the following we absorb the factor  $(1 - 1/D_2)$  into the 122 rate; it will no longer appear explicitly.

Including the resonant-capture terms yields the total time rate of change of  $P_2$  due to  $2e$  transitions.

$$\dot{P}_2 = -2A_{122}(D_1 - P_1)P_2^2 + 2R_{122}P_1(D_2 - P_2)^2. \quad (2)$$

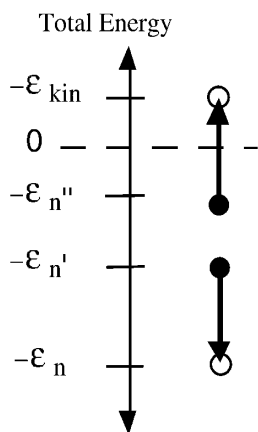


FIG. 1. In an autoionization event of a multiply excited ion, an electron in a higher energy level,  $n''$ , is ejected, while another, in  $n'$ , falls to a lower energy level,  $n$ . Energy conservation requires that  $\varepsilon_{\text{kin}} = \varepsilon_n - \varepsilon_{n'} - \varepsilon_{n''} \geq 0$ . In the two level atomic kinetics system treated in the text  $n'' = n' = 2$ , and  $n = 1$ .

The equation for  $P_1$  is seen to be

$$\dot{P}_1 = +A_{122}(D_1 - P_1)P_2^2 - R_{122}P_1(D_2 - P_2)^2. \quad (3)$$

The conservation rule for integer configuration transitions,  $2N_1 + N_2 = \text{const}$ , is obeyed by Eqs. (2) and (3).

Now Eqs. (2) and (3) are linearly dependent, on account of the conservation rule, so our two-level system requires further constraint in order to yield nontrivial solutions. In the density, temperature, and radiation regimes of many laser-heated plasmas the  $2e$  transition rates are as great as the  $1e$  bound-bound transition rates, while the  $1e$  ionization and recombination rates are smaller. We close the system by augmenting Eqs. (2) and (3) with  $1e$  bound-bound excitation and deexcitation terms.

$$\begin{aligned} \dot{P}_1 = & -P_1(D_2 - P_2)^2 R_{122} + (D_1 - P_1)P_2^2 A_{122} \\ & - P_1(D_2 - P_2)T_{12} + (D_1 - P_1)P_2 T_{21}, \end{aligned} \quad (4)$$

$$\begin{aligned} \dot{P}_2 = & +2(D_2 - P_2)^2 P_1 R_{122} - 2P_2^2 (D_1 - P_1) A_{122} \\ & + (D_2 - P_2)P_1 T_{12} - P_2 (D_1 - P_1) T_{21}. \end{aligned} \quad (5)$$

Here the total one-electron bound-bound transitions between the levels include both collisional and radiative rates;  $T_{12} = C_{12} + R_{12}$ ,  $T_{21} = C_{21} + R_{21}$ .

The  $1e$  bound-bound transitions conserve the total number of electrons in the two levels,  $N_1 + N_2$ , while the  $2e$  transitions conserve  $2N_1 + N_2$ . This provides a path to the solution of the system in steady state; linear combinations of Eqs. (4) and (5) are

$$(\dot{P}_1 + \dot{P}_2) = (D_2 - P_2)^2 P_1 R_{122} - P_2^2 (D_1 - P_1) A_{122}, \quad (6)$$

$$(2\dot{P}_1 + \dot{P}_2) = -P_1(D_2 - P_2)T_{12} + (D_1 - P_1)P_2 T_{21}. \quad (7)$$

In steady state the  $2e$  and  $1e$  processes are separately in balance, and together determine the two level populations:

$$P_1 = D_1/[1 + (A_{122}/R_{122})(T_{12}/T_{21})^2], \quad (8)$$

$$P_2 = D_2/[1 + (A_{122}/R_{122})(T_{12}/T_{21})]. \quad (9)$$

All the preceding development has been guided by the usual treatment of the  $1e$  transitions, and its LTE limit in particular. Let us confirm that if the  $1e$  bound-bound processes obey detailed balance, then the required LTE populations of the two levels are recovered. Using detailed balance

$$\begin{aligned} T_{12}^{\text{LTE}} &= \exp[-(\varepsilon_1 - \varepsilon_2)/T_e] T_{21}^{\text{LTE}}, \\ R_{122} &= \xi \exp[-(\varepsilon_1 - 2\varepsilon_2)/T_e] A_{122}, \end{aligned}$$

we find that indeed

$$P_i^{\text{LTE}} = D_i/1 + \exp[-(\varepsilon_i + \mu)/T_e]. \quad (10)$$

Equations (10) contain the Fermi factors of the temperature,  $T_e$ , level energy,  $\varepsilon$ , and chemical potential,  $\mu$ . The relation between  $R_{122}$  and  $A_{122}$  is always true for a nondegenerate Maxwell-Boltzmann distribution of free

electrons, where  $\xi = (n_e/2)(h/\sqrt{2\pi m_e T_e})^3$  and  $\mu = T_e \ln(\xi)$ .

Observe that as free electron density,  $n_e = Z^* N_i$ , decreases in an LTE plasma, both the lower and the upper level populations decrease proportional to the density,  $P_1^{\text{LTE}} \sim D_1 O(n_e)$  and  $P_2^{\text{LTE}} \sim D_2 O(n_e)$ , on account of  $\mu$ ; examine Eqs. (10). Then the LTE ionization state increases with decreasing density,  $Z^{*\text{LTE}} \approx Z - P_1^{\text{LTE}} \sim Z - O(n_e)$ . This behavior is often observed to be violated, and thus stimulates much NLTE work.

NLTE regimes of  $2e$  transition driven recombination and ionization, “ $2e$  equilibrium” ( $2eE$ ), can be identified according to the ratio of the bound-bound excitation and deexcitation rates which appear in the effective Fermi factors in Eqs. (8) and (9). At modest-to-low density, and in the absence of a strong radiation field, collisional excitation and radiative deexcitation are dominant;  $T_{12} \sim C_{12}$ , and  $T_{21} \sim R_{21}$ . Note that  $A_{122}/R_{122} \sim 1/n_e$ , so that when  $T_{12}/T_{21} \sim C_{12}/R_{21} \sim n_e$ , the smaller upper level population,  $P_2$ , becomes independent of density, while the larger lower level population,  $P_1$ , increases with decreasing density

$$P_1^{2eE} \sim D_1/[1 + O(n_e)],$$

$$P_2^{2eE} \sim D_2/[1 + O(\text{const})].$$

Since  $Z^{*2eE} \approx Z - P_1^{2eE}$ , our average atom model predicts the recombination of laser plasmas as density decreases.

The preceding description is in sharp contrast to the CRE which goes to the coronal limit with decreasing density. Straightforward analysis of the CRE model including only  $1e$  bound-bound and bound-free transitions of the two level system yields

$$P_1^{\text{CRE}} \sim D_1 O(\text{constant}), \quad P_2^{\text{CRE}} \sim D_2 O(n_e).$$

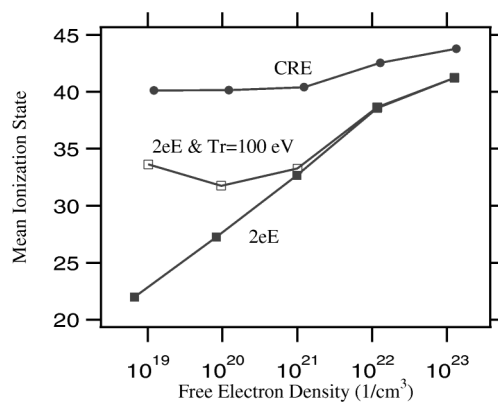


FIG. 2. The average ionization state,  $\langle Z^* \rangle$ , for gold plasmas with  $T_e = 600$  eV and  $T_r = 0$ . The  $2eE$  results exhibit the recombination scaling derived in the text for electron densities below about  $10^{22}/\text{cm}^{-3}$ , and the CRE results exhibit the coronal limit for densities below about  $10^{21}/\text{cm}^{-3}$ . A radiation field of  $T_r = 100$  eV arrests the  $2eE$  recombination for densities below about  $10^{21}/\text{cm}^{-3}$ , but has no appreciable effect on CRE.

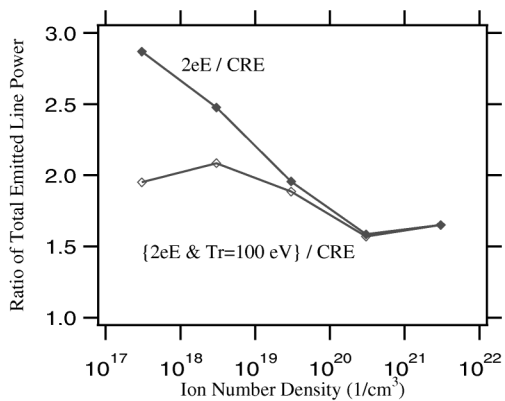


FIG. 3. The ratio of the total power emitted in line radiation by the 2eE and CRE plasmas,  $X_{\text{tot}}^{2eE}/X_{\text{tot}}^{\text{CRE}}$ , from the calculations of Fig. 2.  $X_{\text{tot}}(\text{W}/\text{cm}^3)$  is the sum of all spectral lines  $X_{n'n}$ , as displayed in Fig. 4. The 2eE emissivity always exceeds the CRE by at least 50%, and is partly due to elevated excited level populations as derived in the text.  $X_{\text{tot}}^{2eE}$  is about  $(2 \times 10^{19}, 5 \times 10^{17}, 1 \times 10^{16}, 1 \times 10^{14}, 1 \times 10^{12}) \text{ W}/\text{cm}^3$  from the highest to the lowest density points.

Thus we expect to find that  $P_1^{2eE} > P_1^{\text{CRE}}$ , so that  $Z^{*2eE} < Z^{*\text{CRE}}$ , and also that  $P_2^{2eE} > P_2^{\text{CRE}}$ , so that we also expect to find that the radiated power obeys  $X_{21}^{2eE} > X_{21}^{\text{CRE}}$ .

In a many-level model including  $2e$  transitions, the levels are coupled via all “triples” as illustrated in Fig. 1. Because a level can be any member of a triple, there are both gain and loss terms from both  $R$  and  $A$ . It is also necessary to test the triples against the energetics threshold for  $2e$  transitions. The terms to add to a CRE model to obtain a 2eE model are straightforward to derive from the development above.

Results were computed for “complete” seven-level hydrogenic 2eE and CRE [7] models of gold ( $\text{Au}$ ,  $Z = 79$ ,  $A = 197$ ) plasmas at  $T_e = 600 \text{ eV}$  and  $T_r = 0$  where heuristically the N,O shells correspond to levels 1,2 of the two-level model analyzed. Hydrogenic  $2e$  rates were approximated by extrapolating the collisional-excitation differential cross section below threshold [8].

Figure 2 shows the average ionization,  $\langle Z^* \rangle$ , over a wide range of electron density. The two characteristic scalings of the average ionization state with density are evident and significantly different. We also show the effect of introducing  $T_r = 100 \text{ eV}$  at low density where it acts to arrest the 2eE recombination, but does not appreciably affect the CRE.

The power radiated by the plasma as x rays, its emissivity, comes from the free electron thermal energy; it is an important contribution to the plasma thermal cooling rate. Figure 3 shows that the plasma energy balance implied by the 2eE population scaling is remarkable as well. The 2eE radiative cooling rate greatly exceeds that

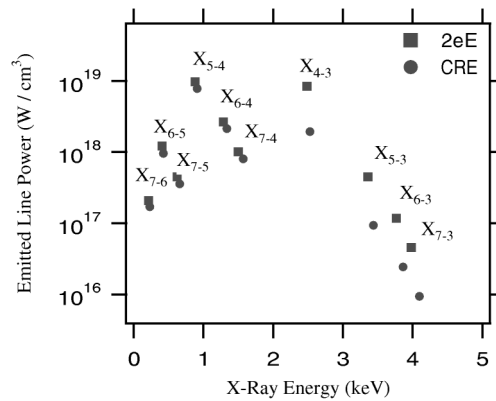


FIG. 4. The line radiation emission spectra,  $X_{n'n}(\text{W}/\text{cm}^3)$  at energy  $\varepsilon_{n'n} = \varepsilon_n - \varepsilon_{n'}$  ( $n' > n$ ; see Fig. 1), of the 2eE and CRE models at the highest density point of Figs. 2 and 3. The sum of  $X_{n'n}$  over all lines, pairs  $n' > n$ , equals the total radiated power of Fig. 3. Here the enhanced emissivity of the 2eE plasma is partly due to  $X_{43}^{2eE}$ , which results from enhanced  $M$ -shell vacancies. This characteristic difference in the spectra ought to be observable in the laboratory.

of the CRE, and is partly due to enhanced excited level populations as shown for the two-level model. This may be expected to have a significant effect on the plasma's hydrodynamical evolution.

Figure 4 shows the 2eE and CRE radiated power spectra for the highest density point of Figs. 2 and 3. The emissivity of the lines  $X_{54}$  and  $X_{43}$  is responsible for the difference in the total emissivity of the two models, and exhibits an observable signature of the underlying NLTE atomic kinetics.

This work was performed under the auspices of the U.S. Department of Energy at the Lawrence Livermore National Laboratory under Contract No. W-7405-ENG-48.

- [1] J.D. Lindl, *Phys. Plasmas* **2**, 3933 (1995).
- [2] R. W.P. McWhirter, *Phys. Rep.* **37**, 165 (1978).
- [3] S.H. Glenzer *et al.*, *Phys. Rev. Lett.* **82**, 97 (1999).
- [4] W.A. Lokke and W.H. Grasberger, Lawrence Livermore Laboratory Report No. UCRL-52276, 1977.
- [5] G.B. Zimmerman and R.M. More, *J. Quant. Spectrosc. Radiat. Transfer* **23**, 517 (1980).
- [6] Y.T. Lee, *J. Quant. Spectrosc. Radiat. Transfer* **38**, 131 (1987).
- [7] S.J. Rose, Council for the Central Laboratory of the Research Councils, Technical Report No. RAL-TR-97-020, 1997.
- [8] R.M. More, G.B. Zimmerman, and Z. Zinamon, in *Atomic Processes in Plasmas*, edited by A. Hauer and A.L. Merts, AIP Conf. Proc. No. 168 (AIP, New York, 1988), p. 33.